Organic Rankine cycle thermal architecture - from concept to demonstration

Angad Panesar*, Robert Morgan, Dave Kennaird
School of Computing Engineering and Mathematics, University of Brighton, U.K
*a.s.panesar@brighton.ac.uk

Keywords
Internal combustion engine
Organic Rankine cycle
Working fluid blend
Heat recovery arrangement
Steady state testing

Highlights

- A versatile heat recovery and working fluid test-rig is presented
- The specific exergy cost consideration supported the direct exhaust gas utilisation
- The water blends offered a noticeable improvement in overall conversion efficiency
- A holistic approach in NOx reduction, downsizing and heat recovery is proposed
- Experimental process parameters corresponded to the near-optimal simulation values

Abstract

Waste heat to power conversion is expected to play a key role in reducing CO_2 emissions in the mid-to-large scale internal combustion engines. The realisation of cost-effective deployment of Organic Rankine Cycles (ORC) is shown to be hindered by several key factors, including, disconnect between parameters considered in simulation studies to those demonstrated experimentally, utilisation of low-grade ORC practice for high-grade applications, challenges in integrating multiple heat recovery sources etc. To address such challenges, a programme of 'concept-to-demonstration' is in progress at the University of Brighton, with the presented focus here being on the thermal architecture.

This paper describes some of the important features of a new experimental ORC test-rig that may contribute towards increased overall conversion efficiencies. These features include, firstly, a variable heat source setup, allowing the potential to replicate a wide range of realistic gaseous sources. Secondly, the direct utilisation of the High-Temperature (HT) exhaust gases, which is expected to lower the specific evaporator exergy cost by 22%. Thirdly, deployment of HT water blends, this is estimated to increase the potential of overall conversion efficiency by 2.4 times. Fourthly, a flexible thermal platform, offering multiple and efficient heat utilisation, with a holistic approach to NOx reduction, downsizing and exhaust heat recovery. Finally, advanced process conditions (e.g. 29.3 bar, 270.9°C), which corresponds to the near-optimal region, and offers the possibility of a 12.5% conversion rate of heat recovered to expansion power. The potential benefits are quantified using a combination of published literature, procurement findings, simulation results (Aspen HYSYS) and preliminary experimental measurements (NI LabVIEW). The paper concludes with the rational for the next intended research effort, i.e. high-pressure ratio and two-phase expansion machines.

Nomenclature

c_p	specific heat (kJ/kg°C)
$\dot{E}$	exergy (kW)
LMTD	log mean temperature difference (°C)
$\dot{m}$	mass flow rate (kg/s)
$\dot{Q}$	energy (kW)
T	temperature (°C)
Greek symbols	
η	efficiency
Δ	difference
Abbreviations	
CAC	charge air cooler
EGR	exhaust gas recirculation
GWP	global warming potential
HEX	heat exchanger
HT	high temperature

ICE	internal combustion engine	46
IHE	internal heat exchanger	47
LT	low temperature	48
MT	medium temperature	49
ORC	organic Rankine cycle	50
PRV	pressure reducing valve	51
UA	product of heat transfer coefficient and area (W/°C)	52
VFR	volume flow ratio	53
Subscripts		54
avg	average	55
evap	evaporator	56
exh	exhaust	57
out	outlet	58
recover	recoverable	59
pp	pinch point (minimum temperature difference between two thermal curves)	60 61

62

63 **1 Introduction**

64 Internal Combustion Engines (ICE) are the dominant prime movers for road, marine and rail freight
65 transportation, and decentralised power generation. Due to their high absolute fuel consumption,
66 they represent a significant challenge in terms of CO_2 emissions reduction. A key global imperative
67 is therefore the substantial improvement of ICE thermal efficiency. To target the portion of the lost
68 fuel chemical energy, technology road maps and reviews support the specific need for waste heat
69 recovery [1, 2]. The heat to power conversion technologies are additionally of particular interest to
70 the process industry and the renewable sector [3, 4]. Heat to power conversion on ICEs has been
71 demonstrated using various methods. However, amongst these, Organic Rankine Cycle (ORC) is
72 stated as one of the preferred technology options when comparing the overall conversion
73 efficiency and its technology readiness level [5, 6].

74

75 Research and development activities have recently become even more relevant due to the
76 automotive sector, where the projected improvements in ICE efficiency are stated to be insufficient
77 to comply with an aggressive CO_2 legislation [7, 8]. The recent developments in key ORC

components are aiming to address this. Prototypes of fin-tube and spiral-tube evaporators have been demonstrated by Yang et al. and Zhang et al., respectively [9, 10]. Numerical and experimental results with isentropic efficiencies of 65% for a two-stage turbine and piston expander have been presented by Seher et al. [11].

The case to implement hydrocarbons and the fourth generation refrigerants is additionally becoming more robust. Using ethanol as the working fluid for a truck application, a fuel consumption improvement of 4.3% has been shown by Edwards et al. [8]. Due to the increased emphasis on Global Warming Potential (GWP), Yang et al. indicated an ultra-low GWP refrigerant (R1234yf) optimal from a thermo-economic point of view for a marine engine [12].

Application specific heat recovery arrangements for ICEs have also been presented. Arunachalam et al. theoretically evaluated five different arrangements, even combining Charge Air Cooler (CAC) heat from a truck engine [13]. Due to the considered engine platform, the power produced from Exhaust Gas Recirculation (EGR) only was 72% compared to the dual-loop arrangement recovering all the three gaseous sources (i.e. exhaust, EGR and CAC). To recover High-Temperature (HT) exhaust and Low-Temperature (LT) coolant heat, Wang et al. proposed a cascade system using R245fa and R134a as the working fluids for the HT and the LT interconnected cycles [14].

Adaptability of ORCs have also led to the proposition of ORCs combined with other technologies. Simulation results by Yılmaz showed that the air conditioning needs of an intercity bus can be realised using the exhaust energy in combination with R134a and R245fa as the working fluids [15]. Shu et al. proposed the use of thermoelectric generator for HT heat recovery, followed by ORC for LT heat recovery in a theoretical study [16].

Despite the advancements, there still exist key challenges hindering the cost-effective deployment of ORCs. Reasons amongst these include, disconnect between parametric values considered in simulation studies to those demonstrated experimentally, utilisation of low-grade ORC practice for high-grade applications, challenges in integrating multiple heat recovery sources in the evolving engine platforms, development of versatile high-pressure ratio expanders (i.e. vapour and two-phase) etc. Extending upon the findings of the recent simulation studies [17, 18], this paper

summarises the year-long effort in 'concept-to-demonstration' of a new experimental ORC test-rig. The scope of the work presented here is limited to the important thermal architecture features that may contribute towards investigating increased overall conversion efficiencies. The paper consists of two main sections, the methodology phase and the demonstration phase, which utilise a combination of published literature, procurement findings, simulation results (Aspen HYSYS V8 [19]) and preliminary experimental measurements (NI LabVIEW 2014 [20]). In the methodology section, focus is given to the rationale behind the heat source setup, utilisation of exhaust gases, the chosen working fluids, process operating conditions and the flexible thermal platform. In the demonstration section, the current capability of the experimental ORC test-rig and the preliminary thermal platform results are presented and discussed. Finally, the paper concludes with the intended research efforts with expansion machines.

2 Methodology phase

2.1 Heat source setup

Figure 1a presents the range of heat quality and the proportion of fuel chemical energy wasted by typical mid-to-large scale ICE (0.2-2 MW) utilising a range of fuels (e.g. bio-diesel, natural gas) and regulated emissions standards (e.g. Euro 6, Tier III). In freight transportation, such engines operate at near-steady state conditions, typically between the mid-speed mid-load point and the engine rated condition. Heat recovery from the post-turbine exhaust remains a primary choice across various engine platforms. Figure 1a also includes the EGR stream, which is a potential secondary choice for heat source. Additionally, the continued trend of cooler engine intake temperatures and higher engine intake pressures now means that, from an exergy perspective, the CAC is also a potential secondary choice in engines operated at relatively high speeds and loads. Figure 1a then illustrates that a suitable heat source setup for testing ORCs must offer a wide range of gaseous heat quality and quantity levels.

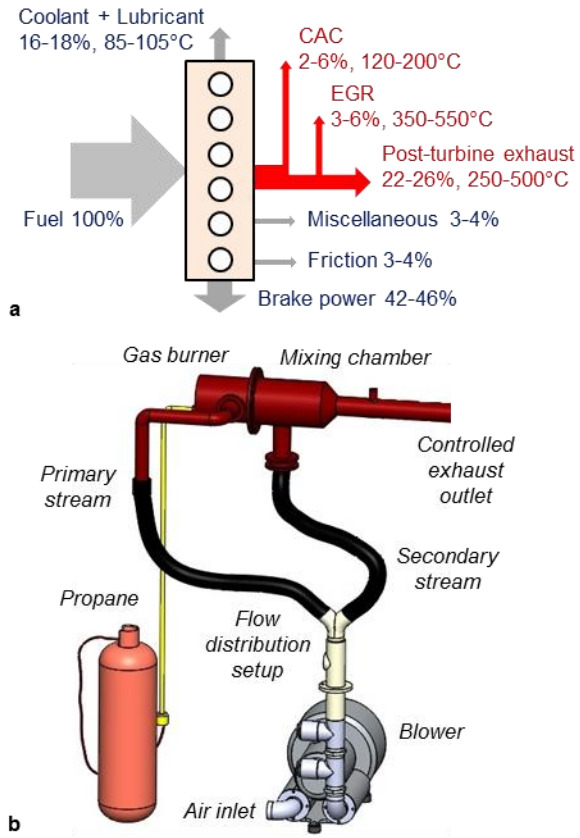

Figure 1 (a) Fuel chemical energy distribution with various regulated emissions standards in a range of mid-to-large scale ICEs at mid-to-high speeds and loads (b) Test-rig section representation of the variable heat source setup

To offer this flexibility, while avoiding the challenge of integrating and operating engine test-beds in parallel, the waste heat was experimentally simulated using a blower (Elmo Rietschle 2BH1 side channel, 0.35 kg/s) and gas burner (Maxon 3" TUBE-O-THERM, 120 kW) combination, as shown by the test-rig section representation in Fig. 1b. The compressed air flow exiting the blower was distributed into two streams, the primary compressed air stream acted as the main air supply to the gas burner, the secondary compressed air stream was used for dilution purposes. This was since, firstly, the burner exhaust gas temperature is typically well above the maximum engine exhaust gas target temperature of 500°C. By utilising the secondary compressed air stream and controlling the quantity of flow using the flow distribution setup (which includes 2 butterfly valves), the net exhaust gas temperature can be controlled. Secondly, the gas burner must be accompanied with a higher pressure air stream since, ambient gas burners either cannot operate when faced with the backpressures that will be introduced by the exhaust heat exchanger (HEX), or produce emissions higher than those required to certify their operational use. As a result, depending on the fuel supply

to the gas burner, quantities of primary and secondary compressed air flows, and the backpressure created by the HEX, this flexible heat source setup has the potential to deliver gaseous heat qualities between 200-500°C and heat quantities between 12-120 kW, at a pressure of 1.05-1.25 bar.

2.2 Utilisation of exhaust gases

To recover the relatively HT exhaust gas heat of ICEs, the approach of using an intermediate thermal-oil loop is often proposed and implemented. As shown in Fig. 2a, the diathermic-oil recovers the HT exhaust gas heat, and transfers it to the ORC working fluid. A similar process integration was also proposed by Shu et al. for automotive heat recovery using conventional refrigerants like R245fa and isopentane [21].

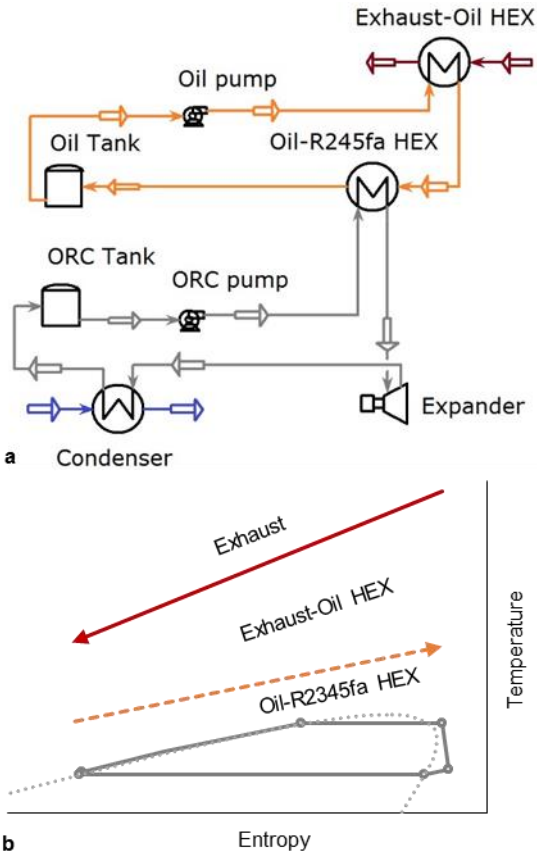

Figure 2 Thermal-oil loop coupled with a conventional LT ORC (a) System schematic (b) T-S sketch

Due to the reduced heat source temperature entering the ORC, the thermal-oil loop approach has two key advantages. Firstly, a reduced risk of thermal degradation in the organic fluid, and

secondly, utilisation of conventional refrigerants and off-the-shelf components for the ORC. If the pressure and temperature limits of the ORC do not change with the addition of the thermal-oil loop, and the maximum available waste heat is transferred to the thermal-oil, then the system power of the ORC will not reduce noticeably. This is since, the total heat transfer losses in the heat recovery process are divided between the two separate HEXs, as illustrated in the temperature-entropy sketch in Fig. 2b.

Unfortunately, the thermal-oil loop approach also introduces a number of disadvantages. The additional sub-system components include the exhaust-oil HEX, the oil tank and the oil pump. Therefore, for roughly equal net power, the system complexity, size, weight and failure points may potentially increase. Furthermore, published literature focused on development activities has indicated that the specific cost of a LT ORC coupled with a thermal-oil loop is expected to be 15% higher when compared to HT exhaust gases being recovered directly in a HT ORC [22].

Operational capability and purchase cost data of numerous HT and LT evaporators in the range of 38-80 kW was compiled during the decision and procurement phase. Table 1 summarises the data for evaporator duty scaled to 50 kW (using £/kW), where Case 1 and 2 represents the LT and the HT ORC approaches, respectively. The comparison was done for an equal quality and quantity of exhaust heat recovered in both cases. When considering the specific energy cost for the ORC evaporator, the HT ORC results in a value 2.8 times higher (42 vs. 116 £/kW). However, such parameters ignore the heat quality available to the working fluid and the additional oil-loop costs, hence, their use should be limited in justifying the LT ORC approach.

Table 1 Data collected to quantify specific energy and exergy costs of the evaporator during the decision and procurement stage

	Case1 Thermal oil + LT ORC	Case 2 HT ORC
Max. oil temp. in ORC evap. (K)	498	-
Min. oil temp. in ORC evap. (K)	393	-
Avg. oil temp. in ORC evap. (K)	443	-
Max. exhaust temp. in ORC evap. (K)	-	673
Min. exhaust temp. in ORC evap. (K)	-	393
Avg. exhaust temp. in ORC evap. (K)	-	521
Cost of the thermal-oil loop system (£)	2350	-
Cost of the ORC evap. (£)	2100	5800
Specific energy cost of the ORC evap. (£/kW)	42	116
Exergy of the heat source in the ORC evap. (kW)	9.1	15.1
Specific exergy cost of the ORC evap. (£/kW)	231.6	383.3
Specific exergy cost of the ORC evap. including thermal-oil loop cost (£/kW)	490.7	383.3

Courtesy of, HTT energy GmbH, ICS Cool Energy, Fulton Ltd., Babcock Wanson UK Ltd., Beverley Environmental Ltd., Shanghai Accessen Group Co., FUNKE GmbH, Graham Corporation, Xylem Inc., Tranter International AB, Vahterus UK Ltd., Baode Heat Exchanger Co., Danfoss Ltd., and Dover Intercompany Services UK Ltd.

As a result, the specific exergy cost for the ORC evaporator (including the thermal-oil loop cost) was considered. The recoverable exergy ($\dot{E}_{recover}$) of the heat in the evaporator ($\dot{Q}_{evap}$) was calculated using the exhaust average temperature ($T_{exh\ avg}$).

$$\dot{E}_{recover} = \dot{Q}_{evap}\left[1 - (T_{radiator}/T_{exh\ avg})\right]$$

Where, $T_{exh\ avg} = (T_{max} - T_{min})/\ln(T_{max}/T_{min})$. Furthermore, $\dot{E}_{recover}$ utilises $T_{radiator}$ (90°C) rather than T_{amb} (20°C), since this represents the thermal limit when considering a realistic engine cooling module. Similarly, the considered T_{max} (400°C) represents the design point limit, rather than the higher engine rated condition (500°C). Despite the higher ORC evaporator cost (£5800 vs. £2100) for the HT ORC approach, the higher exergy available in the ORC evaporator (15.1 kW vs. 9.1 kW) and no additional thermal-oil loop cost (£0 vs. £2350) resulted in a 22% lower specific exergy cost for the ORC evaporator (490.7 vs. 383.3 £/kW).

In addition to the above economic approach, the choice of direct exhaust heat recovery is also supported by the thermodynamic approach. This is since, the thermal-oil loop fails to provide opportunity to reduce the overall system irreversibility. Fundamentally, such systems cannot take full advantage of the HT heat, and mimic LT heat recovery systems. Hence, efforts were focused in

engaging the process industry supply chain in co-designing a HEX for direct exhaust gas and working fluid use.

As a result, a multi-pass welded shell-and-plate HEX, with a heat transfer area and liquid volume of 11.9 m^2 and 0.0126 m^3, was procured from Vahterus UK. The design point parameters include: low fluid and exhaust side pressure drop of 0.19 bar and 0.03 bar; capability to operate under high temperature (380°C) and pressure (40 bar); and average working fluid temperature of 210°C and Log Mean Temperature Difference (LMTD) of 58°C. This HEX is suitable for superheating hydrocarbons and water-hydrocarbon blends.

2.3 Working fluid

Waste heat recovery below 200°C can be considered relatively mature using ORCs with hydrofluorocarbons like R245fa [1, 4]. As a result, these fluids have also been suggested for HT exhaust gas heat recovery, either directly or with a thermal-oil loop. However, they result in lower overall conversion efficiencies due to the lower work potential. To investigate and address this issue, a two-part simulation study was undertaken, firstly to identify suitable working fluids, and secondly to propose a flexible thermal platform.

Recent simulation studies have shown that, alcohols and water-alcohol blends that are not included in widely used fluid data bases like REFPROP 9 can provide an improved case for 250-450°C heat recovery [17]. Amongst the numerous blends, water-propanol blend with water mass fraction between 25-50% can offer a suitable trade-off in view of thermodynamic, thermophysical, chemical, environmental, safety, cost, availability, compatibility, miscibility and decomposition properties.

Utilising the parameters, boundary conditions and assumptions presented in Table 2 (column 1 and 2), which are representative of a truck exhaust heat recovery, Fig. 3 presents the potential of net ORC power against the primary process and sizing parameters for R245fa and water-propanol blend (50/50 by mass). The two process parameters include, firstly, maximum fluid temperature, and secondly, maximum fluid pressure. The two sizing parameters include, firstly, the product of heat transfer coefficient and area per unit of net ORC power (i.e. UA/kW_{net}), and secondly, expansion

volume flow ratio per unit of net ORC power (i.e. VFR/kW_{net}). The utilised ORC energy modelling equations have extensively been published and their repetition is avoided [23-26].

Table 2 Parameters, boundary conditions and assumptions representative of long-haul Euro 6 truck waste heat recovery

Parameters (For Fig. 3 and Table 3)	Values	Parameters (Additional for Table 3)	Values
T_{exh}	400°C	T_{EGR}	500°C
$\dot{m}_{exh}$	0.2 kg/s	$\dot{m}_{EGR}$	0.03 kg/s
$c_{p\,exh}$	1.15 kJ/kg°C	$c_{p\,EGR}$	1.15 kJ/kg°C
$T_{cooling\ air}$	35°C inlet, 55°C exit	$T_{pp\,EGR}$	30°C
$T_{pp\,exh}$	30°C	T_{CAC}	140°C
$T_{condensing}$	90°C	$\dot{m}_{CAC}$	0.19 kg/s
$T_{sub-cooling}$	5°C	$c_{p\,EGR}$	1.01 kJ/kg°C
$T_{superheat}$	5°C	$T_{pp\,CAC}$	10°C
η_{pump}	50%	$T_{pp\,IHE}$	10°C
$\eta_{expander}$	65%		
$\Delta P_{fluid\ side\ all\ HEXs}$	0.1 bar		

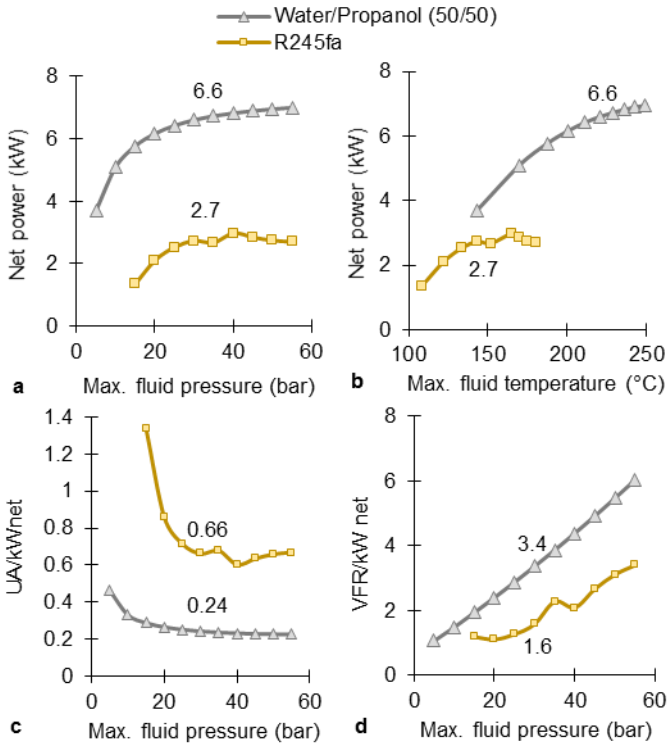

Figure 3 Performance potential comparison between R245fa and water-propanol (50/50). Primary process parameter (a) Maximum fluid pressure (b) Maximum fluid temperature, Primary sizing parameter (c) Indicative overall heat transfer footprint per unit of ORC net power (d) Indicative expansion machine size per unit of ORC net power

Considering the subcritical R245fa operation (Fig. 3a), the 30 bar value was considered near-optimal, offering 2.7 kW of net power for 57 kW of heat recovery ($\eta_{thermal} = 4.7\%$). At the same maximum cycle pressure, the water-propanol blend offered 2.4 times higher net power for a reduced 48 kW of heat recovery ($\eta_{thermal} = 13.8\%$). However, compared to R245fa (Fig. 3b), which required a maximum temperature of around 145°C, the water-propanol blend required a much higher value of 225°C. Both the above primary process parameter results are linked to the relatively higher normal boiling point of the water-propanol blend compared to R245fa (89°C vs. 15°C). When the near-optimal operation of pure propanol and water-propanol blend (50/50) was considered, the temperature/pressure limit of 240°C/25 bar and 245°C/35 bar was established, respectively. The maximum temperature limit was based on a 20°C superheat, such higher superheating margins are essential in transient conditions when using conventional expansion machines.

As a first indicator for the relative heat transfer footprint (Fig. 3c) and expansion machine size (Fig. 3d), UA/kW_{net} and VFR/kW_{net} were considered [27, 28]. With the reduction in the heat transfer footprint being a prime consideration, the water-propanol blend showed a potential of 60% reduction in the overall heat transfer footprint (Fig. 3c). The above parameters then guided the co-design and procurement stage of the desired HT HEX described in the section 2.2. Note that, although Fig. 3d indicates a relative expansion machine size requirement for water-propanol blend being 2.1 times that of R245fa, nonetheless, the absolute VFR requirement was within the reach of piston expanders. Hence, the above results aided the continued examination of water-propanol blend as an alternative. Pure water was not considered for comparison due to its large latent heat and freezing point drawbacks in the current application.

2.4 Thermal architecture

The thermal architecture of ORCs are expected to differ amongst the variety of ICE applications [1, 5]. Hence, a flexible thermal platform with the potential to be modified for either multiple heat recovery and/or efficient heat utilisation is essential for research activities. Figure 4a presents the HYSYS model section of the proposed thermal platform. The red and grey coloured streams correspond to external heat and working fluid, respectively. The heat recovery platform comprises of two LT HEXs in a parallel branched flow followed by one HT HEX. Figure 4b represents the corresponding test-rig section.

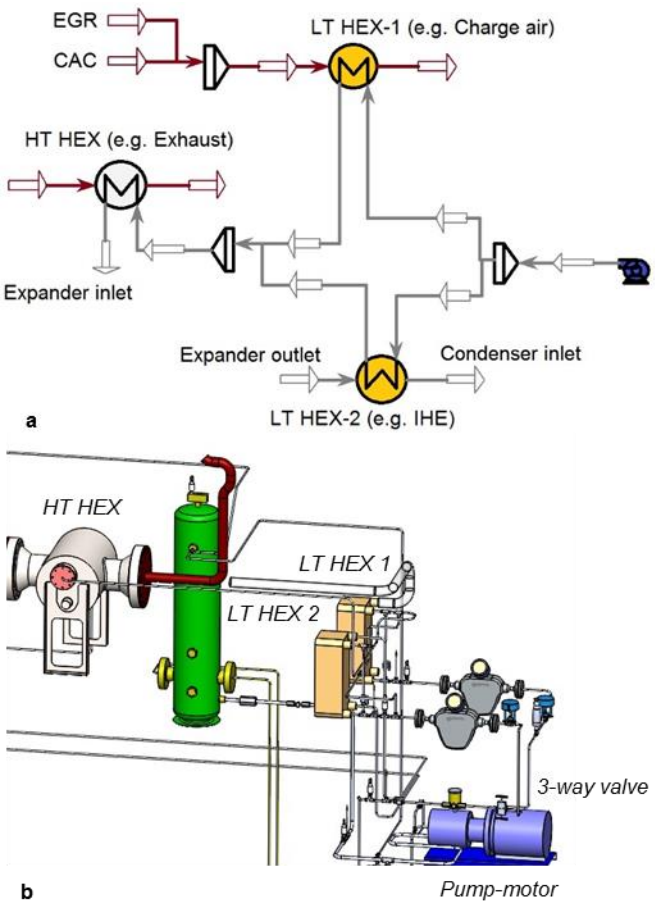

Figure 4 Proposed heat recovery platform with two HEXs in a parallel flow followed by one HEX in series flow (a) HYSYS model (b) Test-rig representation

Using pure propanol as the working fluid, Table 3 summarises the results for comparing the possible heat recovery options. The parameters are normalised to the net heat recovered in the exhaust heat recovery only option. Furthermore, the heat recovery options were targeted for the same net power and with an equal maximum pressure of 25 bar, as stated in section 2.3. For this case study, the earlier used truck exhaust heat recovery parameters (Table 2, column 1 and 2), together with the EGR and CAC parameters (i.e. column 3 and 4) were utilised.

Table 3 Normalised thermal and power values for comparing the different heat recovery options

Heat recovery option	HT HEX	LT HEX-1	LT HEX-2	Fluid	Net power (kW)	Exhaust HEX (kW)	CAC or Combined HEX (kW)	Internal heat exchange (kW)	Condenser (kW)
1	Exhaust	-	-	Propanol	12	100	0	0	88
2A	Exhaust	CAC	-	Propanol	12	86	14	0	88
2B	Exhaust	Combined	-	Propanol	12	66	33	0	87
3	Exhaust	-	IHE	Propanol	12	87	0	12	75

Option 1 from Table 3, i.e. exhaust gas heat recovery only, can be considered as a potential solution where EGR and charge air heat is expected to be minimal. Option 2, i.e. exhaust gas and lower temperature heat recovery, can be deployed in two different cases. Case 2A being where exhaust and charge air heat is recovered in series. Case 2B being where both charge air and EGR heat is mixed and recovered in a combined larger LT HEX located post-compressor followed by exhaust heat in series.

The Ricardo WAVE 2015 [29] model section of the baseline 6-cylinder engine utilised for Case 1 and 2a is presented in Fig. 5a. For brevity, excluded is the after-treatment system, which is used in conjunction with the EGR to meet Euro 6 emissions. The modified engine platform (Fig. 5b) was simulated under the same recirculation rate (15%), engine intake pressure (2.5 bar), temperature (65°C) and fuelling parameters to that of the baseline platform (Fig. 5a). Hence, the regulated emissions are expected to be similar.

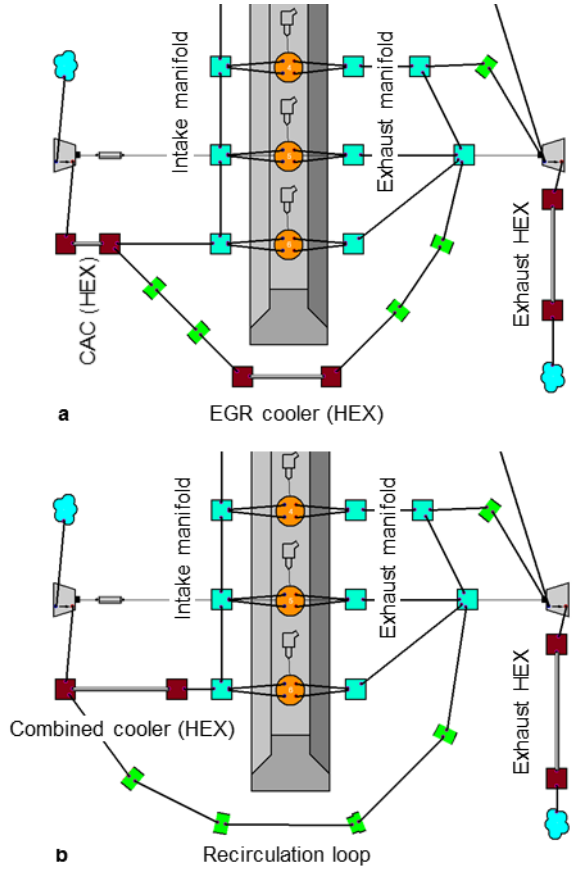

Figure 5 Ricardo WAVE model section of the truck engine platform (a) Typical of current production (b) Proposed holistic NOx reduction, downsizing and heat recovery option

The rational for the case 2B engine architecture is due to the requirement of examining holistic approaches in NOx reduction, downsizing and exhaust heat recovery. The current production of truck engines utilises relatively low rates of EGR. Furthermore, over a wide engine operating map, due to variable rates of EGR and boost pressure, the proportion of EGR and charge air heat are intermittent. As a result, firstly, to recover EGR and exhaust heat in parallel branched flow ORC, relatively low and precise flow rates of working fluid are required in the EGR HEX. This is also a challenge for the three-way flow distribution valve located at the pump exit. Secondly, EGR and charge air heat is available at two different quality levels, creating a further challenge in process integration. From the ORCs perspective, mixing and cooling both the charge air heat and the EGR heat in a common LT HEX may offer three potential advantages. Firstly, reduced number of thermal components, secondly, increased quantity of heat in the LT HEX, and finally, medium quality of heat which is suitable for series heat recovery prior to the exhaust heat. In the simulated case, the heat

source temperature entering the combined HEX was 188°C as a result of mixing the charge air (140°C) and the EGR stream (500°C).

It can be noted that in option 2A (Table 3), which corresponds to series charge air and exhaust heat recovery, the exhaust HEX thermal duty was lowered by 14% for the same level of power output. Furthermore, option 2B, which corresponds to the series combined HEX and exhaust heat recovery, the exhaust HEX thermal duty was lowered by 34% for the same level of power output. The reduced exhaust HEX thermal duty for equal ORC net power in options 2A and 2B was since, the lower temperature exhaust heat recovery was replaced with heat sources that are already a load on the engine cooling module.

Finally, option 3 may be considered for exhaust heat recovery only, but in demanding condenser packaging applications, like the European trucks. In this option, the working fluid was slightly superheated compared to options 1 and 2 (from 215 to 250°C). The level of superheating paired with the drying nature of the working fluid allowed the use of an Internal Heat Exchanger (IHE) to partially recover the exergy that may be lost in the condenser. Due to the internal heat recuperation, the exhaust heat recovery was reduced by 13%, but more importantly, the condenser heat rejection was lowered by 15%. Note that, the presented work has been limited to utilising a maximum of two HEXs during heat recovery. Although more complex arrangements are possible using the three HEXs, it's currently unclear if the added complexity offers any techno-economical benefits.

3 Demonstration phase

3.1 ORC test-rig

Following the two-part simulation study on working fluid (Fig. 3) and flexible thermal platform (Table 3), a range of parametric studies using pure water, water-alcohol blends and pure alcohols were conducted. The overall range of the simulation results were then translated into: system specification and layout, process and instrumentation diagram, and the procurement plan, which acted as the design reference for the experimental ORC test-rig. Due to the prototype nature of the work, control and instrumentation, hazard and operability, and risk assessment studies were undertaken. Noteworthy items included: temperature and pressure limits of gaskets and O-rings; burner emissions under different fuelling and backpressure conditions; independent mechanical

pressure relief valve and pulsation damper; and forced alcohol vapour extractions from enclosed prototype components.

Figure 6 presents the complete test-rig representation at its current status. The test-rig is not aimed at demonstrating the power-density ratio of a commercial system, but is aimed at conducting working fluid research, demonstrating HT ORC operation, guiding development by evaluating components etc. The relatively large foot-print of the test-rig is due to the fact that the balance of the plant was sourced from the process industry to achieve the target variable thermal and pressure rating with high safety margins (e.g. test pressure of 84 bar in the case of the HT HEX). Additionally, the test-rig is built with the aim to characterise components of varying capacities from different industrial sectors, alongside testing different thermal platforms.

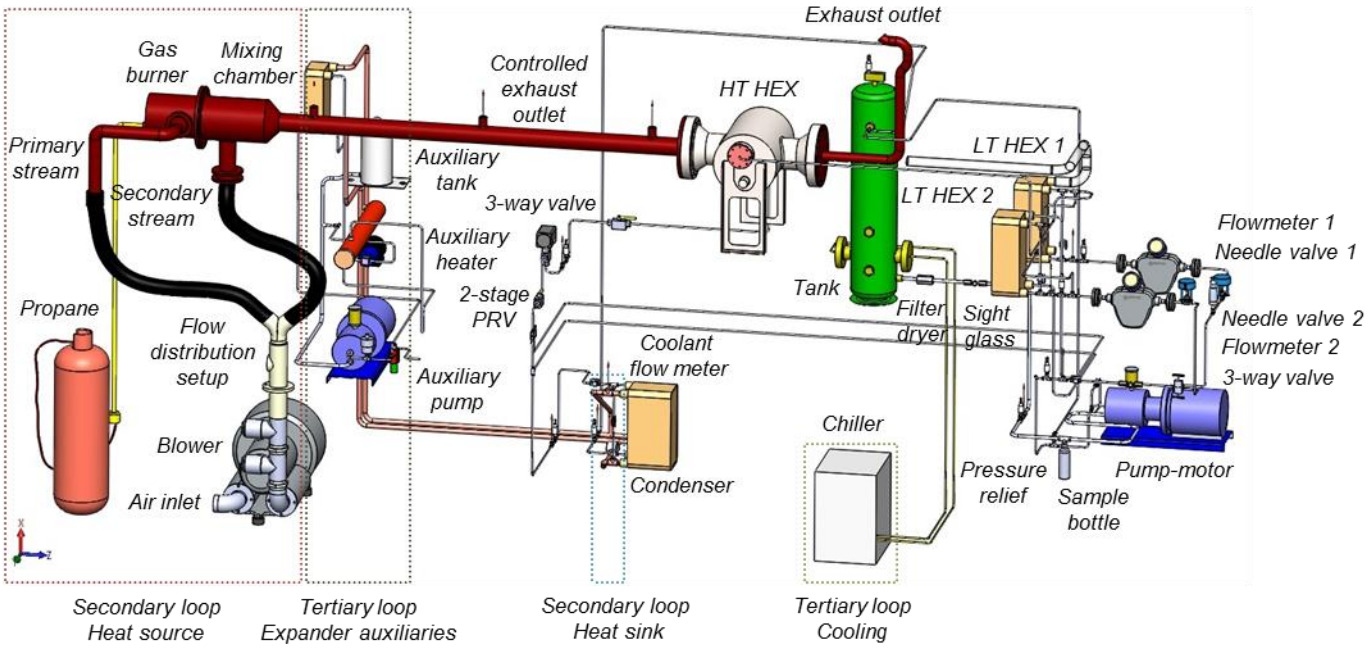

Figure 6 In-house experimental ORC test-rig with three HEXs in mixed series and parallel flow for alcohols and water-alcohol blends utilised in the 'concept-to-demonstration' of the thermal architecture phase of the work

As shown in Fig. 6, the test-rig comprises of five flow loops: ORC fluid, heat source, heat sink, chiller and auxiliaries. The key ORC fluid loop components, following the flow from the pump inlet include: HydraCell pump-motor; Johnson pressure relief valve; HydraCell pulsation damper, HiP 3-way valve; Swagelok needle valve; SWEP brazed plate HEX; Vahterus welded plate and shell HEX; HiP 3-way

valve; Swagelok Pressure Reducing Valve (PRV); SWEP brazed plate condenser and Bitzer liquid receiver tank. In addition, the pump inlet includes, HVAC sight glass and Swagelok particulate filter and Swagelok sample cylinder. This sample line will be utilised in future works to quantify thermal degradation in pure alcohols and water-alcohol blends as a function of time, pressure and temperature exposures.

Considering the pump, the HT HEX, the PRV and the condenser forming the four temperature-pressure quadrants, Table 4 lists further component information, and additionally, summarises the section limits of the test-rig at its current status. The tank pressure limit paired with the sight glass temperature limit provided the capability of up to 9 bar and 85°C at the LP LT section. Whereas, the HT HEX pressure and temperature limits provided the capability of up to 40 bar and 380°C at the HT HP section.

Table 4 ORC fluid loop component information and section pressure-temperature capability limits

Component	Comment/Section limit
ORC pipework	Φ 10 mm (branched parallel flow) to Φ 18 mm (full flow). Continuous orbit welded, pressure tested with 12 bar (LP section) to 45 bar (HP section)
LT HP section	
HydraCell G10 diaphragm pump-motor	-
Johnson 1216HP pressure relief valve	48 bar
HydraCell RD pulsation damper	100°C
HiP 76NFC 3-way manual ball valve	-
Swagelok n-series air-actuated needle valve	-
HT HP section	
SWEP V120T brazed plate HEX	225°C
Vahterus 3HH welded plate and shell HEX	40 bar, 380°C
HiP 76NFC 3-way air-actuated ball valve	-
Swagelok KCY pressure reducing regulator	-
MT LP section	
SWEP B200 brazed plate condenser	-
Bitzer FS liquid receiver tank	9 bar, 120°C
LT LP section	
HVAC JJ sight glass	42 bar, 85°C
Swagelok SS particulate filter	-
Swagelok 304L sample cylinder	-
Aermec Venice20 water cooled chiller	-

The ORC loop pipework, which varied between 10-18 mm in diameter, was continuous orbit welded. A brazed plate liquid cooled condenser was utilised due to its ability to withstand a wider

range of condensation pressures and temperatures. As a result, condensing characteristics relevant to both stationary and mobile ICE applications can be simulated. Furthermore, the tank was modified to receive the chiller loop as a safety measure and as a means to draw down lower boiling point fluids from the system.

3.2 Preliminary experimental results and discussion

Data was captured and logged using CompactRIO and five AI, AO, MIO modules. The Emerson micro-motion Coriolis/density and Flowstat Pelton wheel flowmeters were used for the ORC fluid and coolant loop, respectively. A total of 12 Omega K-type thermocouples and 7 Omega pressure transducers were utilised to derive the thermodynamic conditions at key state points to create the T-S diagram. Table 5 lists further instrumentation information, and additionally, summarises the measurement accuracy and range.

Table 5 ORC test-rig instrumentation, accuracy and range

Instrumentation	Comment
National Instruments LabVIEW 2014	CompactRIO (9074) at a logging rate of 0.01 sec; AI modules (9201, 9203, 9237); AO module (9265); MIO module (9381)
Emerson CMFS050M micro-motion Coriolis flow and density meter	Accuracy of ± 0.25% in the range of 0.018-1.8 kg/s
Omega K-type (KMTXL) thermocouples	6 for working fluid; 4 for heat source; 2 for heat sink
Omega PX1009L0 and PXM35MD pressure transducers	7 for working fluid; Accuracy ± 0.25% (Max. 149°C, 100 bar); Accuracy ± 0.25% (Max. 343°C, 68.9 bar); Pre-calibrated and verified against Druck PV multi-function pump
Flowstat CSD Pelton wheel coolant flowmeter	Accuracy of ± 2% in the range of 0.25-2.5 kg/s

Figure 7a-e presents key process parameters over a 1 minute duration from a steady-state test with the thermal architecture configured as option 1 (Table 3). Steady-state was defined as a 3 minute duration where the change in fluid at the HT HEX exit was limited below 2.5°C and 0.75 bar from a set target value. The exhaust temperature at the inlet and exit of the HT HEX was 385.1 and 248.7 °C (Fig. 7a), while the water-glycol coolant temperature at the inlet and exit of the condenser was 50 and 57.1 °C (Fig. 7b). In the initial demonstrations presented here, deionised water (97% by mass) was used as the working fluid to demonstrate the high temperature and pressure operational capability. The reason to utilise water was to facilitate commissioning and system development

prior to introducing alcohols in the system. Note that, the test-rig is fully compatible with a wide range of alcohols and their water blends.

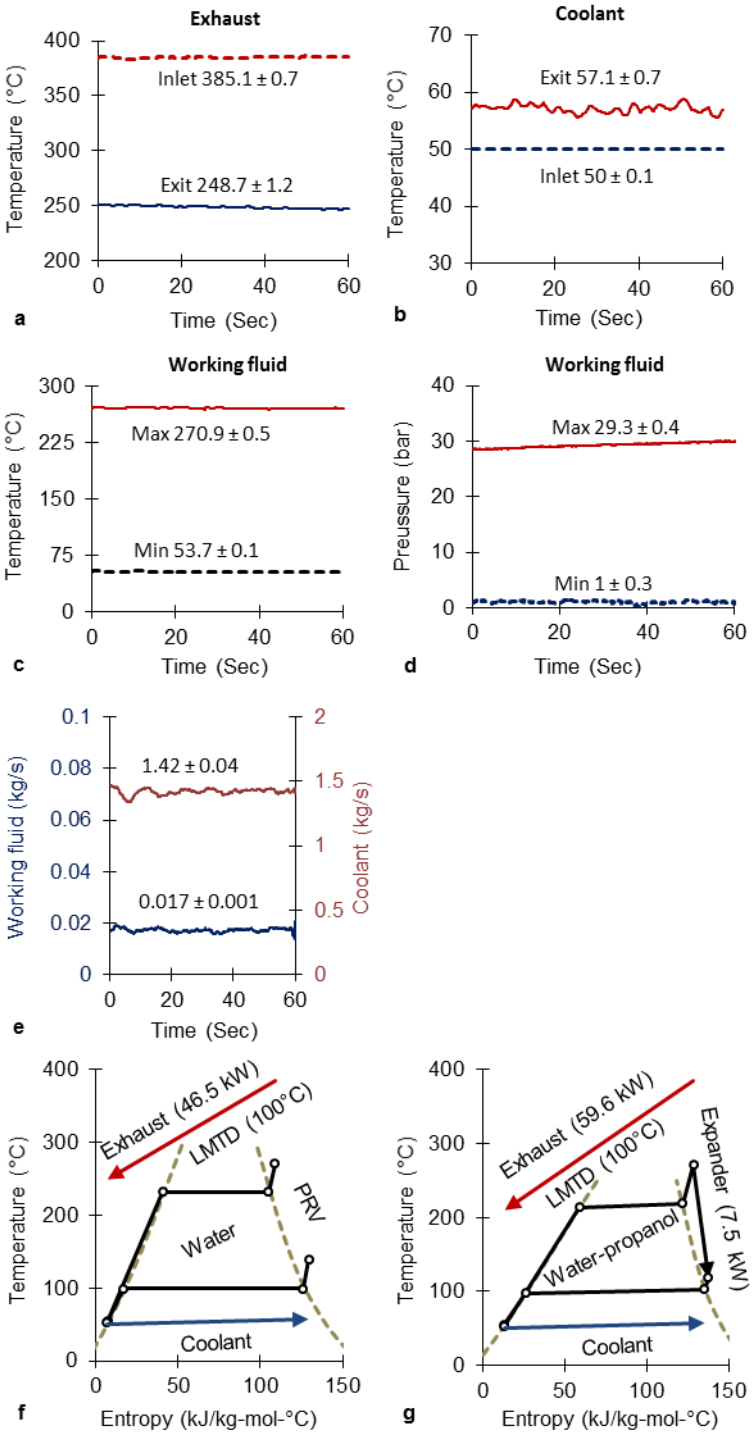

Figure 7 Off-design steady-state demonstration test results as option 1 arrangement (a) Source quality (b) Sink quality (c) Fluid temperature limits (d) Fluid pressure limits (e) ORC fluid and coolant flow rates (f) T-S diagram of the process using a PRV (g) Potential T-S diagram when utilising water-propanol blend paired with a high-pressure ratio expansion process

453 The HT HEX exit temperature (270.9 °C, Fig. 7c) and pressure (29.3 bar, Fig. 7d) was targeted to be
454 comparable to that required by the water-propanol blend in Fig. 3. To simulate the inlet and exit
455 pressures of the high-pressure ratio expander, which will be required under HT differential ORCs, a
456 PRV was utilised. Furthermore, the successful demonstration of throttling via the PRV is critical. This
457 is since, under start-up and transient conditions, which may correspond to two-phase at the HT HEX
458 exit, the flow needs to be by-passed when using conventional expanders and turbines. With a fluid
459 flow rate of 0.017 kg/s (Fig. 7e), an average of 46.5 kW of heat was recovered in the HT HEX
460 (Fig. 7f). Compared to the thermal design point of the test-rig, the preliminary tests were simulated
461 at a relatively benign heat source condition, since the aim was to demonstrate stable operation. A
462 result of the off-design condition can be seen in Fig. 7f, where high level of working fluid reserve
463 was available in the tank, contributing to the high sub-cooling.
464
465 Figure 8a-e presents key process parameters from another 1 minute duration from a steady-state
466 test, but with the thermal architecture being configured as option 2B (Table 3), i.e. combined cooler
467 heat recovery by the LT HEX. The exhaust temperature at the inlet of the HT HEX was 395.7 °C,
468 whereas, the temperature at the inlet and exit of the LT HEX was 190.5 and 112.8 °C (Fig. 8a). These
469 values were targeted to be comparable to the 188°C and 115°C simulation values from section 2.4.
470 The coolant inlet and exit temperature was 20.5 and 46.4 °C (Fig. 8b). The fluid maximum/minimum
471 temperature and pressure of 216.1/35.8 °C, 19.9/0.9 bar was achieved at a flow rate of 0.016 kg/s
472 (Fig. 8c-e). The resulting T-S diagram of this process is presented in Fig. 8f. Note that, the parallel
473 branched flow (Fig. 6) is fully instrumented, hence a further option is possible in which both the LT
474 HEXs are utilised by controlling the flow via the 3-way valve at the pump exit.

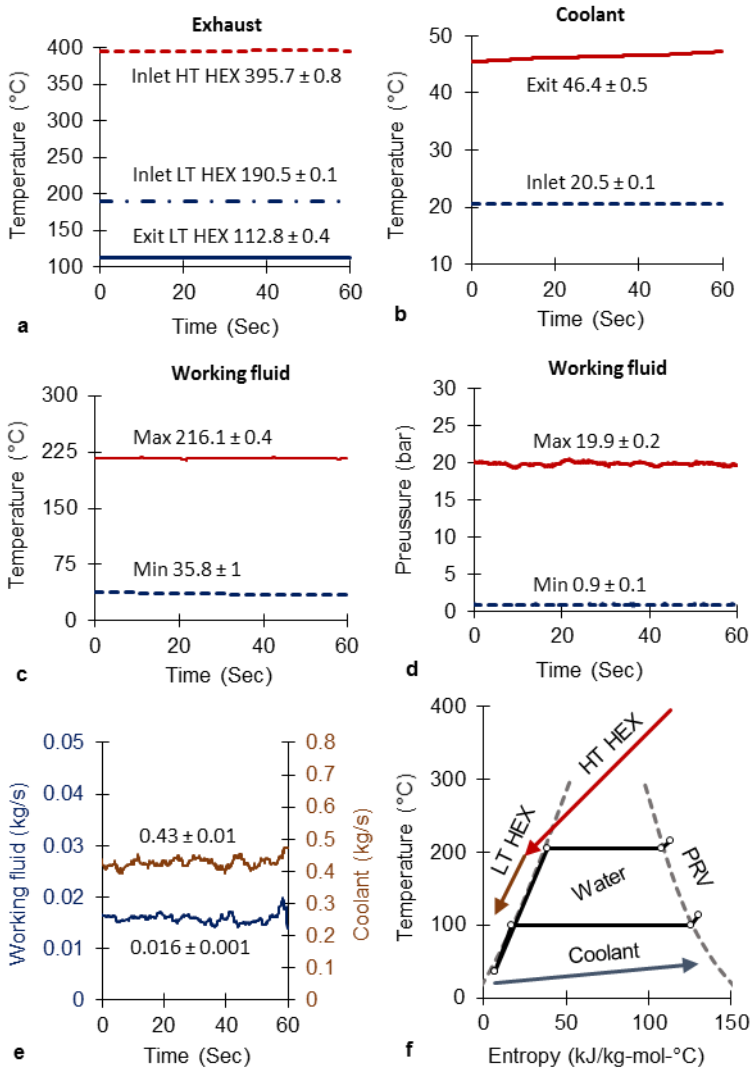

Figure 8 Off-design steady-state demonstration test results as option 2B arrangement (a) Source quality (b) Sink quality (c) Fluid temperature limits (d) Fluid pressure limits (e) ORC fluid and coolant flow rates (f) T-S diagram of the process using a PRV

3.3 Power generation potential

To estimate the recoverable power for the steady-state demonstration test condition, the experimental measurements of option 1 were utilised in the ORC model. The PRV was replaced with a 65% efficient two-stage expander with a pressure ratio of 4.6:1 each. Additionally, the working fluid was also replaced to the water-propanol blend. Figure 7g shows the resulting T-S diagram of the ORC, which offered a potential expander power of 7.5 kW for 59.6 kW of heat recovery. The generated expander power using water-propanol blend was 12% higher when compared against pure water. This was since, assuming a similar LMTD value in the HT HEX, the blend recovered higher quantities of exhaust heat (59.6 vs. 46.5 kW). This was principally due to the

tailored, and rather reduced, latent heat of vaporisation of the water-propanol blend compared to pure water. This also supports in explaining why water has been suggested as a working fluid for heat source qualities above 500°C [1, 5], and will in fact offer lower overall conversion efficiencies for typical exhaust heat recovery. Finally, assuming similar heat to expansion power conversion rate as that of Fig. 7g, the ORC test-rig can be tailored for efficient expansion machines up to 15 kW.

The 'concept-to-demonstration' of the thermal architecture, as summarised in this paper, concludes the first phase of the activity. Figure 3d and 7g also highlight the next key phase of the activity, i.e. investigation of high overall expansion ratio machines. To this effort, it can be noted that the test-rig (Fig. 6) includes four expander auxiliary components (pump, heater, tank, HEX) which can be adapted for lubrication and cooling of expansion machines during development. With the added potential of tolerating two-phase expansion, the next key phase of the activity is expected on reciprocating expanders. The ability of an expansion machine to operate under high-pressure differentials and with varying fluid phases results in, increased average power in transient conditions and increased heat recovery in reduced heat quality conditions [17], boding the case for ORC in challenging applications.

4 Conclusion

A programme of 'concept-to-demonstration' is underway at the University of Brighton to investigate some of the challenges hindering the widespread adoption of ORCs. With a focus on, heat source setup, utilisation of exhaust gases, working fluid, process operating conditions and heat recovery platform, this paper has summarised the methodology and demonstration phase of activity relating to the thermal architecture. The current key features of the experimental ORC test-rig which may contribute towards investigating reduced system costs and increased overall conversion efficiency can be summarised as:

Variable heat source setup: Offering the potential of research and development for a wide capacity range of components under realistic ICE conditions. This is since, the blower-burner setup can be tailored for heat qualities and quantities between 200-500°C and 12-120 kW, respectively.

Direct exhaust heat utilisation: Projected to reduce the specific evaporator exergy cost by 22% when compared to a LT ORC coupled with a thermal-oil loop. Furthermore, the reduction in components and complexity, for equal net power, is vital in mobile applications.

Water-alcohol blends: Estimated to increase the potential of overall conversion efficiency by 2.4 times when compared to a system utilising R245fa. This additionally guides the rationale for the need of new ORC practice in HT applications.

Flexible thermal platform: Utilisation of two LT-HEXs in the parallel branch flow followed by the one HT-HEX that can be configured for multiple and/or efficient heat utilisation for a variety of ICE applications. Additionally, a holistic approach (by using combined HEX) to NOx reduction (by recovering EGR heat), downsizing (by recovering charge air heat) and exhaust heat recovery is proposed in the case of truck engines. The combined cooler and exhaust heat recovery can then reduce the additional heat rejected by the engine cooling module by 34% for an equal net power when compared to exhaust heat recovery only option.

Advanced process conditions: Demonstrated stable working fluid pressure (29.3 bar) and temperature (270.9°C) capability corresponding to the near-optimal region identified by the simulation studies. When considering water-propanol blend, this offers the heat recovered to expansion power potential of 12.5%.

The 'concept-to-demonstration' of the thermal architecture concludes the first phase of the activity. Investigations using reciprocating expanders operating under high-pressure differentials and with varying fluid phases will be the focus of future works.

Acknowledgements

The construction of the ORC test-rig presented in this paper was principally funded by the Innovate UK (101566) and the University of Brighton's strategic investment. The contributions of Emily Pike-Wilson and Richard Sansome are noted.

Reference

1. Sprouse III, C. and C. Depcik, Review of organic Rankine cycles for internal combustion engine exhaust waste heat recovery. Applied Thermal Engineering, 2013. 51(1–2): p. 711-722.
2. Stanton, D.W., Systematic Development of Highly Efficient and Clean Engines to Meet Future Commercial Vehicle Greenhouse Gas Regulations. SAE Int. J. Engines, 2013. 6(3): p. 1395-1480.

3. Nafey, A.S. and M.A. Sharaf, Combined solar organic Rankine cycle with reverse osmosis desalination process: Energy, exergy, and cost evaluations. Renewable Energy, 2010. 35(11): p. 2571-2580.
4. Tchanche, B.F., et al., Low-grade heat conversion into power using organic Rankine cycles - A review of various applications. Renewable and Sustainable Energy Reviews, 2011. 15(8): p. 3963-3979.
5. Saidur, R., et al., Technologies to recover exhaust heat from internal combustion engines. Renewable and Sustainable Energy Reviews, 2012. 16(8): p. 5649-5659.
6. Weerasinghe, R., R. Stobart, and S. Hounsham, Thermal efficiency improvement in high output diesel engines a comparison of a Rankine cycle with turbo-compounding. Applied Thermal Engineering, 2010. 30(14-15): p. 2253-2256.
7. Wang, T., et al., A review of researches on thermal exhaust heat recovery with Rankine cycle. Renewable and Sustainable Energy Reviews, 2011. 15(6): p. 2862-2871.
8. Edwards, S., et al., Waste Heat Recovery: The Next Challenge for Commercial Vehicle Thermomanagement. SAE Int. J. Commer. Veh., 2012. 5(1): p. 395-406.
9. Yang, F., et al., Parametric optimization and performance analysis of ORC (organic Rankine cycle) for diesel engine waste heat recovery with a fin-and-tube evaporator. Energy, 2015. 91: p. 128-141.
10. Zhang, Y.-Q., et al., Development and experimental study on organic Rankine cycle system with single-screw expander for waste heat recovery from exhaust of diesel engine. Energy, 2014. 77: p. 499-508.
11. Seher, D., et al., Waste Heat Recovery for Commercial Vehicles with a Rankine Process, in 21st Aachen Colloquium Automobile and Engine Technology, October 8-12, Aachen, Germany. 2012.
12. Yang, M.-H. and R.-H. Yeh, Thermo-economic optimization of an organic Rankine cycle system for large marine diesel engine waste heat recovery. Energy, 2015. 82: p. 256-268.
13. Arunachalam, P.N., et al., Waste Heat Recovery from Multiple Heat Sources in a HD Truck Diesel Engine Using a Rankine Cycle - A Theoretical Evaluation. 2012, SAE International, 10.4271/2012-01-1602.
14. Wang, E.H., et al., Performance analysis of a novel system combining a dual loop organic Rankine cycle (ORC) with a gasoline engine. Energy, 2012. 43(1): p. 385-395.

15. Yılmaz, A., Transcritical organic Rankine vapor compression refrigeration system for intercity bus air-conditioning using engine exhaust heat. Energy, 2015. 82: p. 1047-1056.
16. Shu, G., et al., Parametric and exergetic analysis of waste heat recovery system based on thermoelectric generator and organic rankine cycle utilizing R123. Energy, 2012. 45(1): p. 806-816.
17. Panesar, A., Waste Heat Recovery Using Fluid Bottoming Cycles For Heavy Duty Diesel Engines. 2015, PhD. thesis. School of Computing, Engineering and Mathematics, University of Brighton, DOI: 10.13140/RG.2.1.4559.0248.
18. Morgan, R., et al., A comparative study between a Rankine cycle and a novel intra-cycle based waste heat recovery concepts applied to an internal combustion engine. Applied Energy, 2016. 174: p. 108-117.
19. Aspen Technology Software, HYSYS version 8. 2015.
20. National Instruments, LabVIEW. 2014.
21. Shu, G.Q., et al., Simulations of a Bottoming Organic Rankine Cycle (ORC) Driven by Waste Heat in a Diesel Engine (DE). 2013, SAE International, 10.4271/2013-01-0851.
22. Guillen, D., et al. Development of a Direct Evaporator for the Organic Rankine Cycle. in TMS Annual Meeting, February 27 - March 3, San Diego, USA. 2011.
23. Lakew, A.A. and O. Bolland, Working fluids for low-temperature heat source. Applied Thermal Engineering, 2010. 30(10): p. 1262-1268.
24. Tchanche, B.F., et al., Fluid selection for a low-temperature solar organic Rankine cycle. Applied Thermal Engineering, 2009. 29(11–12): p. 2468-2476.
25. Karellas, S., A. Schuster, and A.-D. Leontaritis, Influence of supercritical ORC parameters on plate heat exchanger design. Applied Thermal Engineering, 2012. 33–34(0): p. 70-76.
26. Li, W., et al., Effects of evaporating temperature and internal heat exchanger on organic Rankine cycle. Applied Thermal Engineering, 2011. 31(17–18): p. 4014-4023.
27. Braimakis, K., et al., Low grade waste heat recovery with subcritical and supercritical Organic Rankine Cycle based on natural refrigerants and their binary mixtures. Energy, 2015. 88: p. 80-92.
28. Shu, G., et al., Alkanes as working fluids for high-temperature exhaust heat recovery of diesel engine using organic Rankine cycle. Applied Energy, 2014. 119: p. 204-217.
29. Ricardo Software, WAVE version 8.1. 2015.